J Sol-Gel Sci Technol (2007) 43:179–185
DOI 10.1007/s10971-007-1565-3

ORIGINAL PAPER

Luminescent characteristics and microstructures of Sr_2CeO_4 phosphors prepared via sol–gel and solid-state reaction routes

Chung-Hsin Lu · Chung-Tao Chen

Received: 27 October 2006 / Accepted: 28 February 2007 / Published online: 6 April 2007

Abstract Blue-light-emitting Sr_2CeO_4 phosphors were synthesized via a sol–gel process and the conventional solid-state method in this study. The developed sol–gel process lowered the synthesis temperature of monophasic Sr_2CeO_4 to as low as 900 °C. In comparison with the solid-state derived powders, the sol–gel derived powders had more uniform morphology and smaller particle sizes. In addition, sol–gel derived Sr_2CeO_4 displayed higher luminescent intensity than that prepared via the solid-state route under the same heating conditions. This is attributed to the improved compositional homogeneity and crystallinity in the sol–gel process. During the heating processes, Sr_2CeO_4 tended to thermally decompose at elevated temperatures. This decomposition reaction resulted in the formation of an impurity phase- $SrCeO_3$ and thereby a decrease in the luminescent intensity. For obtaining Sr_2CeO_4 phosphors with high luminescent intensity, the heating conditions in both processes need to be well modulated.

Keywords Luminescence · Sr_2CeO_4 · Sol–gel · Phosphor

1 Introduction

Much attention has been paid to oxide-based luminescent materials for exploring their luminescence properties. Oxide-based materials appear to be the focus of extensive research interest in the past few decades because of their good stability upon excitation by electron beam [1]. The popularity of oxide-based luminescent materials is due to the fact that they exhibit superior photoluminescence (PL) and cathodoluminescence (CL) properties which make them useful as important components of color emission in field emission displays (FEDs), plasma display panel devices, and lamps [2–5]. Among these luminescent materials, Sr_2CeO_4 is a promising one for FEDs and lamps due to its efficient luminescence under ultraviolet, cathode ray, and X-ray excitation [6–9]. Sr_2CeO_4 has an orthorhombic structure, which consists of one-dimensional chains of edge-sharing CeO_6 octahedra linked by strontium ions [6]. This structure of Sr_2CeO_4 can absorb energy by itself and acts as a sensitizer to transfer the absorbed energy to the luminescence centers—CeO_6 octahedra responsible for the occurrence of blue emission [10]. The luminescence of Sr_2CeO_4 is considered to originate from charge-transfer (CT) transition [11].

Sr_2CeO_4 powders are usually prepared via a conventional solid-state route which generally requires prolonged heating at elevated temperatures and thus results in coarsening of the obtained powders [7–11]. Other methods, such as the co-precipitation process and sol–gel method using PEG polymer, have been used to synthesize Sr_2CeO_4 [12, 13]. However, high-temperature heating is still required in these processes for obtaining pure Sr_2CeO_4. Yu et al. utilized the citrate-gel method to prepare Sr_2CeO_4 [14] and detected the presence of an impurity phase-Ce_4SrO_7 phase in Sr_2CeO_4 powders because of insufficient homogeneity of the starting materials. In order to improve the drawbacks of the previous processes, a sol–gel method employing citric acid (CA) and ethylene glycol (EG) was developed in this study for synthesizing Sr_2CeO_4 powders. CA forms stable metal-ion complexes, and their polyesterification

C.-H. Lu (✉) · C.-T. Chen
Department of Chemical Engineering, National Taiwan University, No.1, Sec. 4, Roosevelt Road, Taipei 106, Taiwan, R.O.C.
e-mail: chlu@ntu.edu.tw

with EG produces polymeric resins [15, 16]. Immobilization of metal complexes in rigid organic polymer networks is considered to decrease segregation of metal ions, thereby improving the compositional homogeneity in the starting materials of Sr_2CeO_4. Therefore, the formed metal complex will enhance the formation of Sr_2CeO_4 and suppress the formation of impurity phases. Increasing the CA/metal ion molar ratio was reported to produce more carboxylic group and polymer resin and enhance the formation of pure phases [16]. The CA/metal ion and CA/EG molar ratio were also found to significantly vary the microstructures of the prepared materials [17, 18]. On the other hand, the combustion method has also been applied to synthesize Sr_2CeO_4 [19, 20]. This method is an alternative wet-chemical method. It is an exothermic reaction and occurs with the evolution of heat. This process is different from the sol–gel process because fuels and oxidizers are required during combustion reactions and no polymerization reactions occur. The effects of the oxidant-to-fuel ratio was found to greatly affect the phase formation [20]. Recently the above sol–gel process has been applied to a spray pyrolysis process for preparing particles with fine size and regular morphology [21].

In this study, Sr_2CeO_4 powders were prepared via both the sol–gel route and solid-state reaction method. The luminescent properties and microstructures of the powders derived from the above two methods were compared. The relation between the luminescent intensity and calcination conditions was also investigated. The sol–gel method was found to improve the microstructures and luminescent properties of the obtained powders.

2 Experimental

Sr_2CeO_4 was prepared via the sol–gel method using CA as the chelating agent and EG as the polymerizing agent. Stoichiometric amounts of strontium nitrate, cerium nitrate hexahydrate, and citric acid monohydrate were dissolved in deionized water with constant stirring. The solution was stirred for 1.5 h, followed by adding EG. The molar ratio of EG: CA: metal ions was set to be 4:2:1. The prepared solution was heated at 130 °C on a hot plate for 1.5 h and later heated at 300 °C until the dried gels were formed. The resulting gels were calcined at 500 °C in air for 2 h at a heating rate of 10 °C/min, and the obtained powders were ground thoroughly. Subsequently, the samples were calcined at various temperatures in air for 4 h at a heating rate of 10 °C/min. For the synthesis of Sr_2CeO_4 via the solid-state method, stoichiometric amounts of strontium carbonate and cerium oxide were ball-milled for 12 h in ethyl alcohol using zirconia balls. The mixed powders were then heated in air at various temperatures.

The obtained Sr_2CeO_4 powders from both methods were characterized via X-ray diffraction (XRD) analysis using Cu-K radiation (λ = 1.54180 Å) (MAC Science, MXP3). The microstructures of Sr_2CeO_4 prepared via the sol–gel and solid state methods were examined via scanning electron microscopy (SEM) (Hitachi S-800 Field Emission Scanning Electron Microscope). A differential scanning calorimeter (Netzsch, DSC 404) was used to analyze the sol–gel derived precursors. The voltage used in SEM analysis was 20 kV. The PL spectra were recorded at room temperature via a fluorescence spectrophotometer (Hitachi F-4500) using a Xenon lamp as an excitation source.

3 Results and discussion

3.1 Formation and decomposition of Sr_2CeO_4

Sr_2CeO_4 powders prepared via the solid-state route were heated at temperatures between 700 and 1,400 °C in air for 4 h, and the products were characterized via XRD analysis (Fig. 1). The relations between the intensity of the main diffraction peaks for each phase and the heating temperature are illustrated in Fig. 2. It is shown in Fig. 1 that only starting materials were observed at 700 °C, indicating no occurrence of reactions. When the mixed powders were

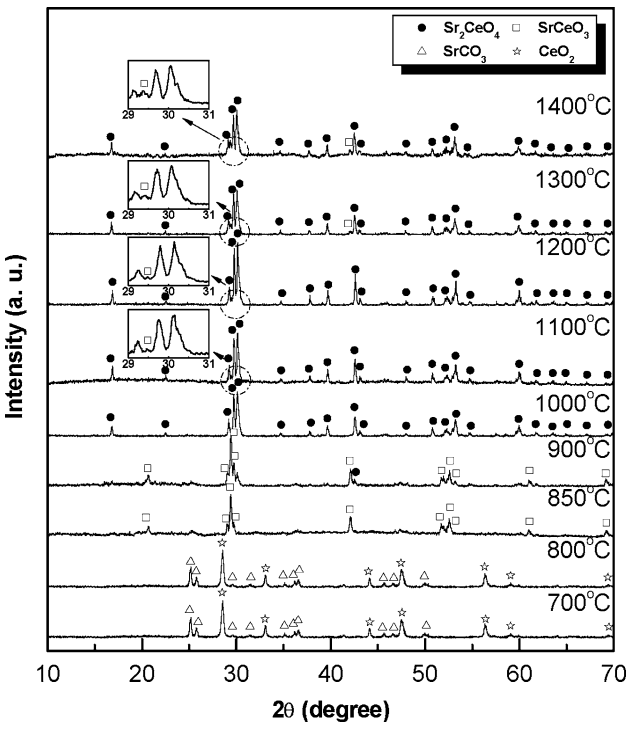

Fig. 1 X-ray diffraction patterns of the starting materials of Sr_2CeO_4 calcined at various temperatures for 4 h in the solid-state reaction process

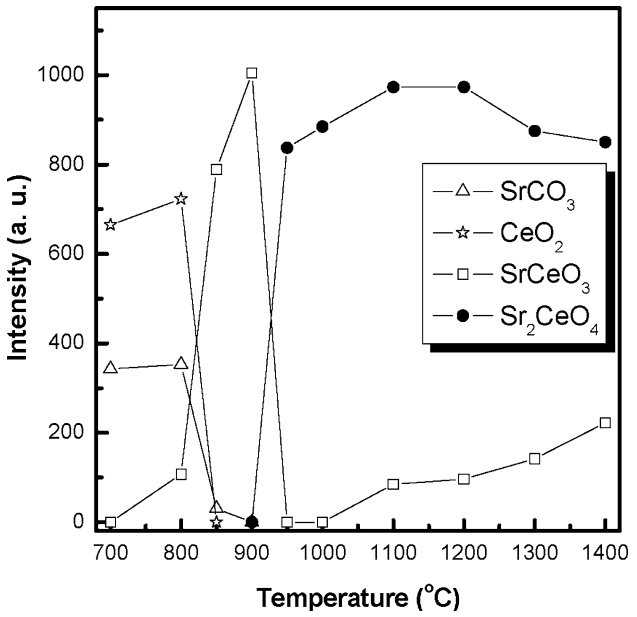

Fig. 2 Diffraction intensity of the resultant phases versus calcination temperature for the starting materials of Sr_2CeO_4 heated at elevated temperatures in the solid-state reaction process

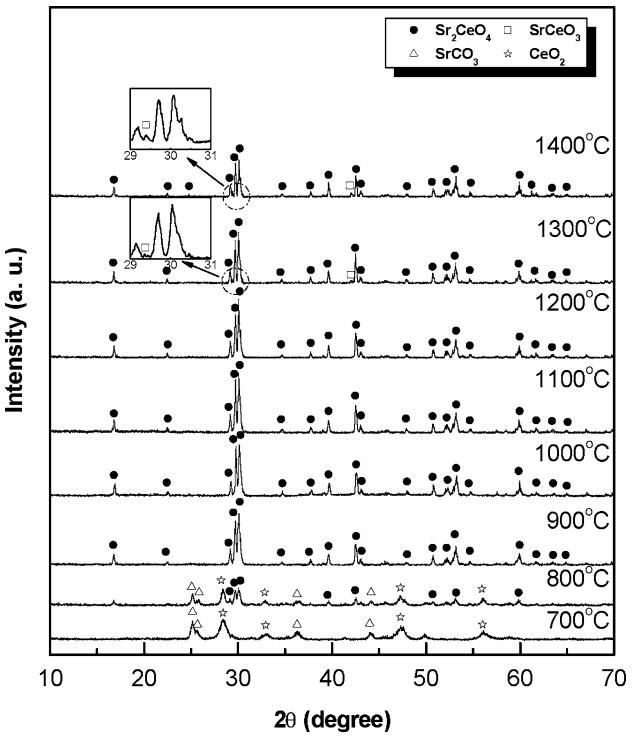

Fig. 3 X-ray diffraction patterns of the sol–gel derived precursors of Sr_2CeO_4 calcined at various temperatures for 4 h

heated at 850 °C, the diffraction peaks of an intermediate phase-$SrCeO_3$ were found. Further raising the heating temperature led to an increase in the amount of $SrCeO_3$. When the heating temperature reached 1,000 °C, $SrCeO_3$ was transformed into Sr_2CeO_4 completely and the target compound was obtained. However, as the heating temperature was raised to 1,100 °C, $SrCeO_3$ reappeared as seen in Fig. 1. This indicates that increasing heating temperature resulted in decomposition of Sr_2CeO_4 to form $SrCeO_3$. Further raising the heating temperature led to greater decomposition of Sr_2CeO_4.

The precursors of Sr_2CeO_4 derived from the sol–gel method were calcined at various temperatures for 4 h. The XRD patterns of the heated powders are illustrated in Fig. 3. The relations between the diffraction intensity of the major peak for each phase and the calcination temperature are illustrated in Fig. 4. $SrCO_3$ and CeO_2 were observed at 700 °C. As the heating temperature was increased to 800 °C, Sr_2CeO_4 began to appear. It is noted that no $SrCeO_3$ was formed prior to the appearance Sr_2CeO_4. After heating at 900 °C, pure Sr_2CeO_4 phase was formed and the recorded diffraction patterns matched well with the standard ICDD pattern (No. 89-5546) [22]. The DSC analysis for the sol–gel derived precursors was performed, and the curve is illustrated in Fig. 5. It was found that an endothermal peak started from 800 °C, and its peak temperature occurred at around 900 °C. The temperature range of this peak matched with the temperature range for the formation of Sr_2CeO_4.

The formation temperature of pure Sr_2CeO_4 in the sol–gel process is lower than that in the solid-state reaction

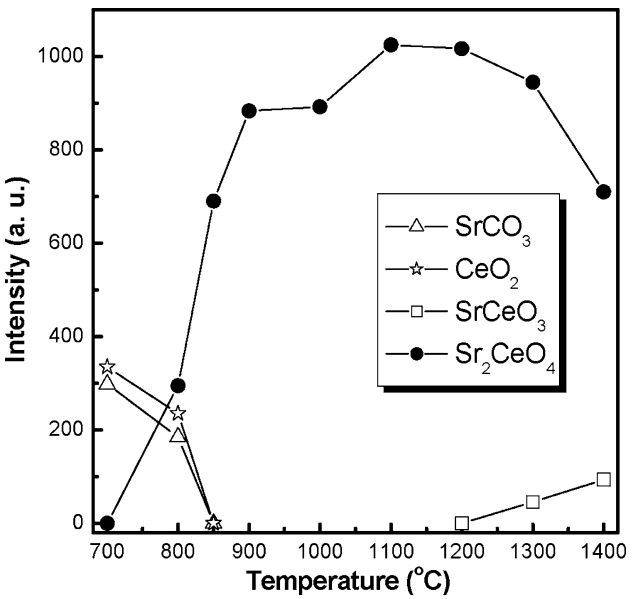

Fig. 4 Diffraction intensity of the resultant phases versus calcination temperature for the precursors of Sr_2CeO_4 heated at elevated temperatures in the sol–gel process

process. Pure Sr_2CeO_4 was present when heating temperature was raised from 900 to 1,200 °C. As the heating temperature reached above 1,200 °C, the diffraction intensity of Sr_2CeO_4 gradually decreased along with an

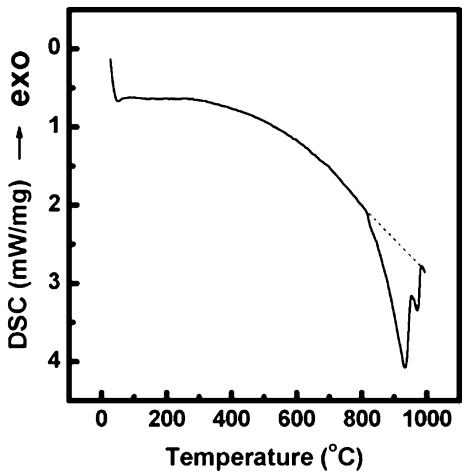

Fig. 5 DSC analysis of the precursors of Sr_2CeO_4 prepared by the sol–gel process

increase in the diffraction intensity of $SrCeO_3$. This phenomenon indicates thermal decomposition of Sr_2CeO_4 at elevated temperatures.

These results clearly demonstrate that the sol–gel method used in this study can successfully synthesize the pure phase of Sr_2CeO_4 at temperature as low as 900 °C, which is much lower than that required in the chemical coprecipitation method reported by Masui et al. [7]. The CA used can form stable metal-ion complexes, and the polyesterification between the formed complexes and EG results in the formation of polymeric resins. As a result, immobilization of metal-ion complexes in such rigid organic polymeric networks reduces segregation of particular metal ions and thereby ensures compositional homogeneity [23]. Therefore, pure Sr_2CeO_4 oxides can be synthesized from the sol–gel derived powders at low temperatures in this study.

It is also found that the solid-state derived Sr_2CeO_4 was readily decomposed to $SrCeO_3$ at 1,100 °C. On the other hand, the sol–gel derived Sr_2CeO_4 had enhanced thermal stability as compared to the solid-state derived samples. The exact decomposition temperature of Sr_2CeO_4 has not been reported in literature. According to the XRD patterns shown in Fig. 1, pure Sr_2CeO_4 seemed to be formed in the 1,000 °C-heated powders in the solid-state processes. However, it is believed that a small amount of the impurity phase-$SrCeO_3$ coexisted in this sample. This tiny amount of $SrCeO_3$ was beyond the detection of XRD analysis, so that no $SrCeO_3$ could be found. The product of the thermal decomposition of Sr_2CeO_4 is $SrCeO_3$. This impurity phase-$SrCeO_3$ in the solid-state derived powders serves as nuclei, and these nuclei can trigger the decomposition reactions at low temperatures. As a result, the thermal stability of the solid-state derived Sr_2CeO_4 is diminished.

3.2 Microstructures of Sr_2CeO_4 powders

The microstructures of the solid-state derived Sr_2CeO_4 are shown in Fig. 6a, b. As shown in Fig. 6a, the grain size of 1,000 °C-heated Sr_2CeO_4 was around 0.8 μm. With a rise in the heating temperature, the grain size of the powders gradually increased. When the heating temperature reached 1,300 °C, significant coarsening of grains was observed with the grain size increased to around 2 μm. As shown in Fig. 6b, the grain shape became irregular and a large number of small particles were formed. The microstructures of sol–gel derived Sr_2CeO_4 are shown in Fig. 6c, d. The 1,000 °C-heated sample had uniform morphology and the grain size was around 0.4 μm which was smaller than of that of the solid-state derived powders. As the temperature was raised to 1,300 °C, the agglomeration of grains occurred with the grain size increased to around 1.5 μm. From the above results, it is noted that the sol–gel process can produce Sr_2CeO_4 with smaller grain size and uniform morphology.

3.3 Luminescent properties of Sr_2CeO_4 powders

The emission spectra of Sr_2CeO_4 powders prepared via the solid-state method are illustrated in Fig. 7. The emission spectra were recorded with an excitation wavelength of 282 nm. When the sample was heated 900 °C, a very weak peak was observed. After heating at 1,000 °C, a broad emission peak was found at 471 nm which is resulted from Ce^{4+} ($4f^0$) to O^{2+} ($2p^6$) charge transfer transition [6]. This emission is attributed to the transition from metal-to-ligand charge-transfer excited state to the ground state [24]. When the heating temperature was raised above 1,000 °C, the emission intensity reversely decreased due to the decomposition of Sr_2CeO_4 at elevated temperatures. Once the decomposition of Sr_2CeO_4 occurred, $SrCeO_3$ was formed. According to the study reported by Goubin et al. [25], $SrCeO_3$ does not have luminescence properties. Therefore, the decomposition reaction resulted in a reduction in the emission intensity of Sr_2CeO_4.

The excitation spectra of solid-state derived Sr_2CeO_4 powders are illustrated in Fig. 8. The excitation spectra were measured at an emission wavelength of 471 nm. When the sample was heated 900 °C, the excitation peak was very weak. When the samples were heated at elevated temperatures, two excitation peaks were observed at 282 and 340 nm. These peaks were due to the interaction of the central Ce^{4+} ion with neighboring oxygen ligands in CeO_6 octahedra leading to ligand-to-metal charge-transfer transition. These two excitation peaks are attributed to two excitation states arising from ligand molecular orbitals $t_{1g} \rightarrow f$ and $t_{1u} \rightarrow f$ charge transfer states [24]. The highest excitation intensity was found in the 1,000 °C-he-

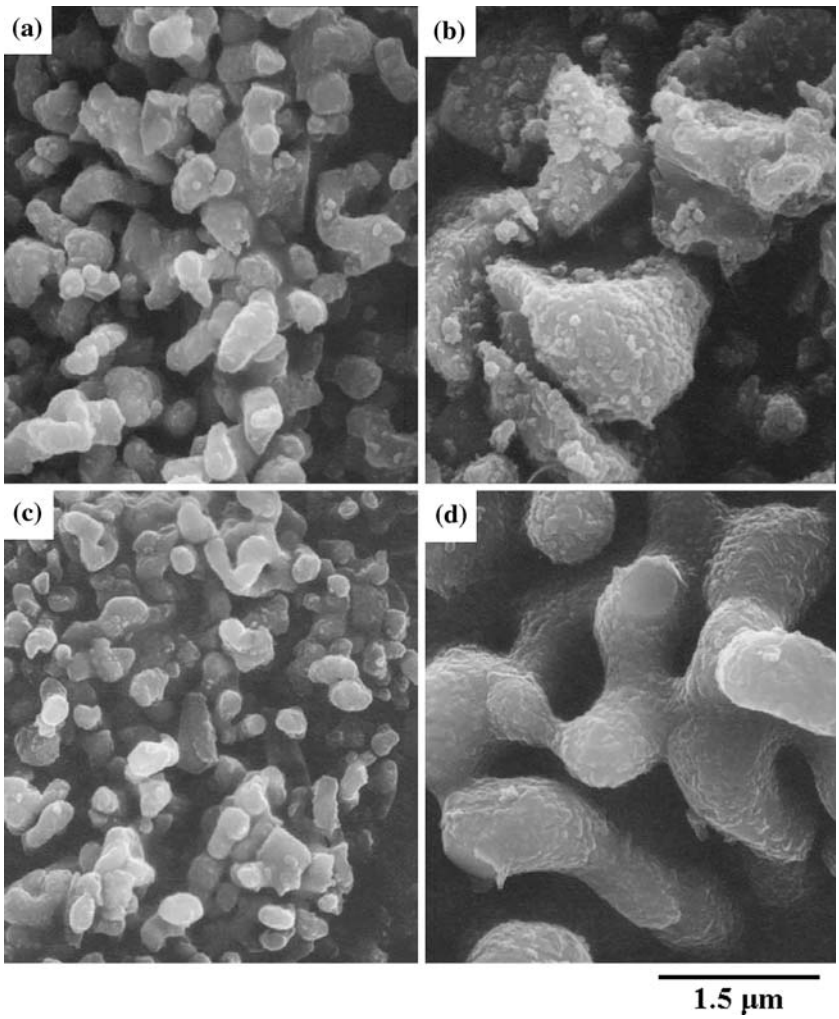

Fig. 6 Scanning electron micrographs of the solid-state derived Sr_2CeO_4 heated at (**a**) 1,000 °C and (b) 1,300 °C for 4 h, and the sol–gel derived Sr_2CeO_4 heated at (**c**) 1,000 °C and (**d**) 1,300 °C for 4 h

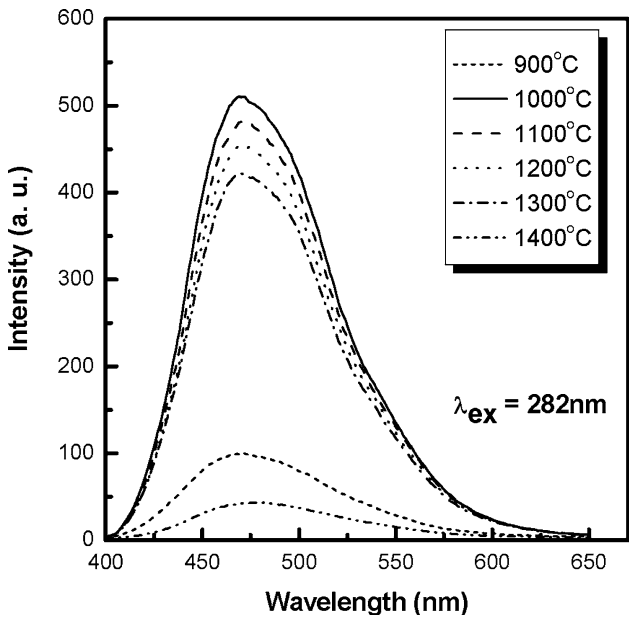

Fig. 7 Emission spectra of Sr_2CeO_4 prepared via the solid-state route

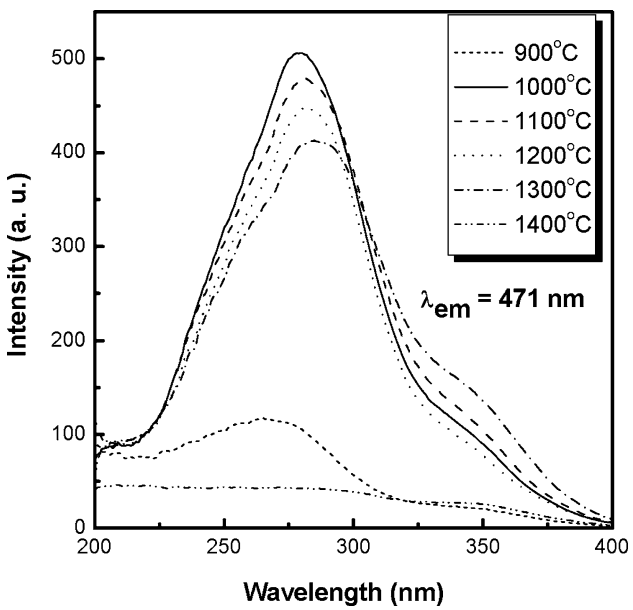

Fig. 8 Excitation spectra of Sr_2CeO_4 prepared via the solid-state route

ated sample. Further increasing temperature led to a decrease in the excitation intensity.

The emission spectra of sol–gel derived Sr_2CeO_4 powders are illustrated in Fig. 9. All emission bands showed a peak at 471 nm due to the transition from metal-to-ligand charge-transfer excited state to the ground state. The highest emission intensity was found in the 1,200 °C-heated sample. As the heating temperature reached above 1,200 °C, thermal decomposition of Sr_2CeO_4 occurred to lead to a decrease in the emission intensity. It is worth noting that the sol–gel method resulted in higher emission intensity as compared with the solid-state method under the same heating conditions. The increase in luminescence intensity is attributable to the improved compositional homogeneity and enhanced crystallinity in the sol–gel process [4, 26, 27]. The excitation spectra of sol–gel derived Sr_2CeO_4 are shown in Fig. 10. The highest excitation intensity was found in the 1,200 °C-heated sample. It was also found that there were red shifts in the excitation spectra when the heating temperatures were increased. This phenomenon is considered to be related to the decomposition Sr_2CeO_4 at elevated temperatures. The thermal decomposition will result in the compositional deviation, thereby affecting the excitation spectra. The effects of the composition on the luminescence properties of Sr_2CeO_4 will be investigated in details.

The effects of thermal decomposition of Sr_2CeO_4 on the luminescence intensity are shown in Fig. 11. The decomposition ratio of Sr_2CeO_4 is defined as $I_{SrCeO_3}/(I_{Sr_2CeO_4}+I_{SrCeO_3})$, where $I_{Sr_2CeO_4}$ and I_{SrCeO_3} represent the diffraction intensities of the major peaks of Sr_2CeO_4 and $SrCeO_3$,

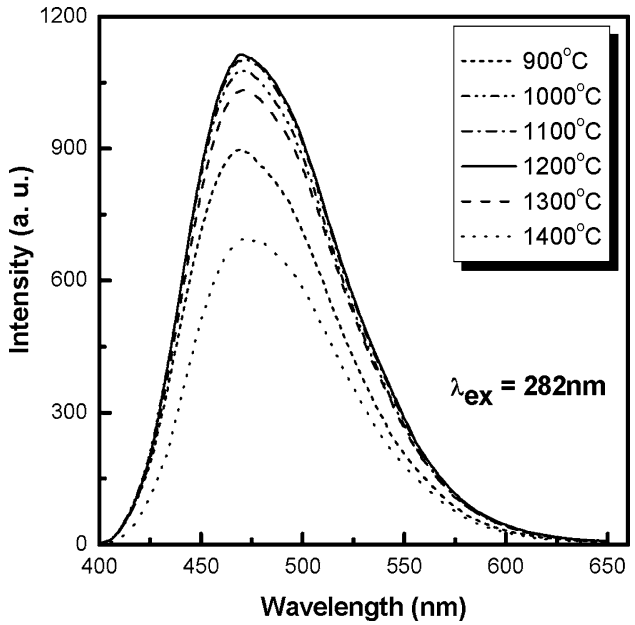

Fig. 9 Emission spectra of Sr_2CeO_4 prepared via the sol–gel route

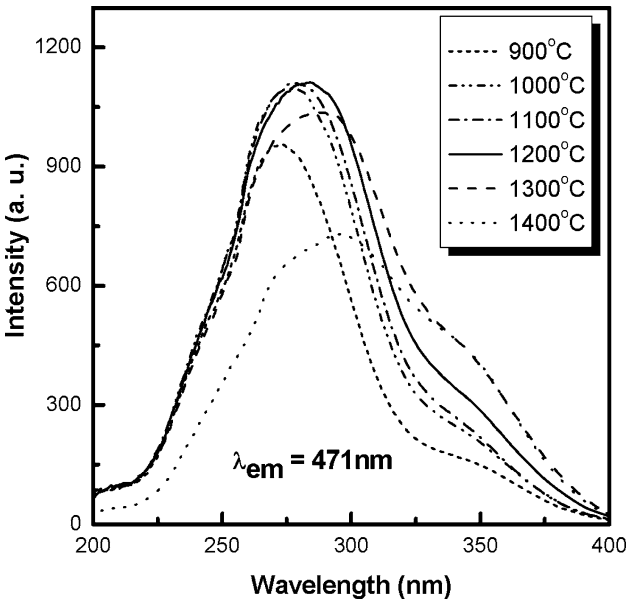

Fig. 10 Excitation spectra of Sr_2CeO_4 prepared via the sol–gel route

respectively. The figure indicates that as the decomposition ratio of Sr_2CeO_4 increases, the luminescence intensity of Sr_2CeO_4 correspondingly decreases in both processes. It is realized that the thermal decomposition of Sr_2CeO_4 at elevated temperatures directly causes the luminescence

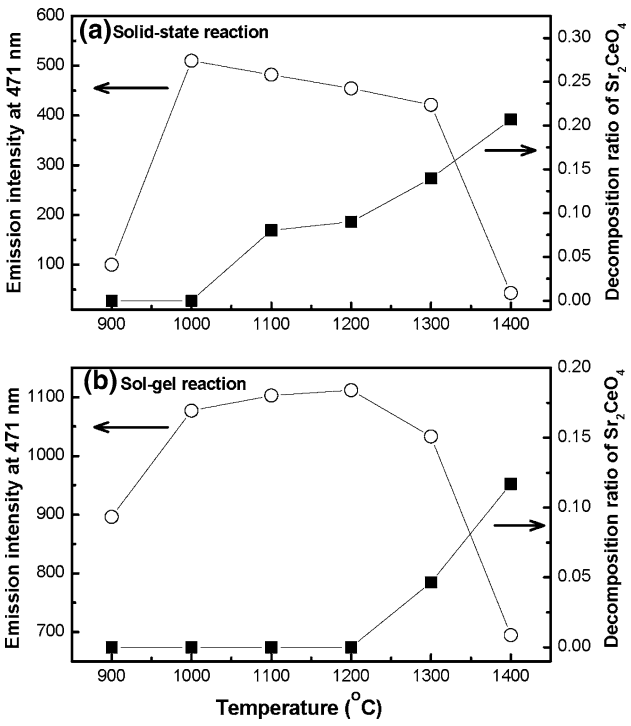

Fig. 11 Decomposition ratio of Sr_2CeO_4 and emission intensity at 471 nm of the samples calcined at various temperatures. (**a**) The solid-state derived samples and (**b**) the sol–gel derived samples

intensity to reduce. As demonstrated in Figs. 7 and 9, raising the temperature up to the decomposition temperature can increase the luminescent intensity because of the enhanced reaction and improved crystallinity of Sr_2CeO_4. However, increasing temperature causes more Sr_2CeO_4 to decompose once the heating temperature is above the decomposition temperature, thereby resulting in a reduction in the luminescent intensity. Based on the above results, it is known that the heating conditions in both processes need to be well modulated for obtaining Sr_2CeO_4 phosphors with high luminescent intensity.

4 Conclusions

Sr_2CeO_4 phosphors were successfully prepared via the sol–gel method using CA and ethyl glycol. The developed sol–gel process resulted in the formation of pure Sr_2CeO_4 at 900 °C. The formation temperature of pure Sr_2CeO_4 in the sol–gel process was lower than that in the solid-state reaction process. The sol–gel derived powders had more uniform morphology and smaller particle sizes than the solid-state derived powders. The sol–gel route resulted in higher luminescent intensity of Sr_2CeO_4 than the solid-state route when the precursors were treated under the same heating conditions. This is ascribed to the improved compositional homogeneity and enhanced crystallinity in the sol–gel process. Sr_2CeO_4 tended to thermally decompose at elevated temperatures and formed an impurity phase-$SrCeO_3$. This decomposition reaction caused the luminescent intensity of Sr_2CeO_4 to decrease. The synthesis and luminescent properties of Sr_2CeO_4 were explored in this study, and these results can serve to provide better understanding for preparing Sr_2CeO_4 with high luminescent intensity and for its future application in luminescence devices.

Acknowledgments The authors would like to thank Dr. K. Krishnan and Dr. B. Bhattacahrjee for helpful discussion. We would also like to thank Mrs. C. Y. Lin for her assistance on SEM. The authors would also like to thank National Science Council of the Republic of China, Taiwan for financially supporting this research under contract No. NSC 95–2221-E002-345-MY3.

References

1. Jiang YD, Zhang F, Summers CJ (1999) Appl Phys Lett 74:1677
2. McKittrick J, Shea LE, Bacalski CF, Bosze EJ (1999) Displays 19:169
3. Phosphor Research Society (1998) Phosphor Handbook. CRC Press, Washington DC
4. Lu CH, Hsu WT, Huang CH, Godbole SV, Cheng BM (2005) Mater Chem Phys 90:62
5. Blasse G, Grabmaier BC (1994) Luminescent materials. Springer-Verlag, Berlin
6. Danielson E, Devenney M, Giaquinta DM, Golden JH, Haushalter RC, McFarland EW, Poojary DM, Reaves CM, Weinberg WH, Wu XD (1998) Science 279:837
7. Masui T, Chiga T, Imanaka N, Adachi G (2003) Mater Res Bull 38:17
8. Perea N, Hirata GA (2005) Opt Mater 27:1212
9. Perea N, Hirata GA (2006) Thin Solid Films 497:177
10. Hirai T, Kswamura Y (2004) J Phys Chem B 108:12763
11. Pieterson LV, Soverna S, Meijerink A (2000) J Electrochem Soc 147:4688
12. Masui T, Chiga T, Imanaka N, Adachi GY (2003) Mater Res Bull 38:17
13. Chen SJ, Chen XT, Yu Z, Hong JM, Xue Z, You XZ (2004) Solid State Commun 130:281
14. Yu X, He XH, Yang SP, Yang X, Xu X (2003) Mater Lett 58:48
15. Xu Y, Yuan X, Lu P, Huang G (2006) Mater Chem Phys 96:427
16. Xu Y, Lu P, Huang G, Zeng C (2006) Mater Chem Phys 95:62
17. Yang WD, Chang YH, Huang SH (2005) J Eur Ceram Soc 25:3611
18. Mariappan CR, Galven C, Crosnier-Lopez MP, Berre FL, Bohnke O (2006) J Solid State Chem 179:450
19. Gomes J, Pires AM, Serra OA (2004) Quim Nova 5:706
20. Chavan SV, Tyagi AK (2004) J Mater Res 11:3181
21. Hong SK, Ju SH, Koo HY, Jung DS, Kang YC (2006) Mater Lett 60:334
22. ICDD Powder Diffraction File, Card No 89-5546
23. Saengkerdsub S, Im HJ, Willis C, Dai S (2004) J Mater Chem 14:1207
24. Nag A, Kutty TRN (2003) J Mater Chem 13:370
25. Goubin F, Rocquefelte X, Whangbo MH, Montardi Y, Brec R, Jobic S (2004) Chem Mater 12:662
26. Kahihana M, Yoshimura M (1999) Bull Chem Soc Jpn 72:1427
27. Lu CH, Hsu WT, Dhanaraj J, Jagannathan R (2004) J Eur Ceram Soc 24:3723